Article ID: 1003－6326(2005)04－0813－05

Processing map for hot working of as extruded AZ31B magnesium alloy①

HUANG Guang-sheng(黄光胜), HUANG Guang-jie(黄光杰),
WANG Ling-yun(汪凌云), PAN Fu-sheng(潘复生)
(College of Materials Science and Engineering, Chongqing University,
Chongqing 400044, China)

Abstract: The deformation behavior of AZ31B magnesium alloy as extruded under hot compression conditions was characterized in the temperature range of 200－400 ℃ and strain rate range of 0.001－1 s^{-1}. The processing maps were obtained at different strains. The results show that the map exhibits flow instabilities as two domains. The domain at beyond 300 ℃ and strain rate of 1 s^{-1} appears with a peak efficiency of power dissipation about 56% occurring. This domain is expected to happen in a hot process, such as hot rolling, hot extrusion and hot forging. There is high efficiency of power dissipation at temperature beyond 350 ℃ and strain rate 0.001 s^{-1}. Such domains suggest the occurrence of superplastic deformation.

Key words: magnesium alloy; AZ31B; processing map; hot deformation; flow instability
CLC number: TG 301 **Document code:** A

1 INTRODUCTION

In recent years, the technique of processing map is very beneficial for optimizing hot workability and controlling the microstructure during hot working. The basis and principles of this approach were described early and its application to the hot working of a wide range of materials was demonstrated[1-3]. A processing map is the superimposition of a power-dissipation map with an instability parameter on a process variable space (strain rate, temperature). In this paper, a short description was introduced.

In brief, the processing map consists of a superimposition of two maps. The first one is a power dissipation map which represents the manner in which the power is dissipated by the material through microstructural changes, the rate of which is represented by a dimensionless parameter called efficiency of power dissipation[4], namely

$$\eta = \frac{2m}{m+1} \tag{1}$$

where m is the strain rate sensitivity index of flow stress. m can be obtained as[5]

$$m = \left.\frac{\partial \ln \sigma}{\partial \ln \dot{\varepsilon}}\right|_{\varepsilon, T} \tag{2}$$

Over this power dissipation map is superimposed an instability map, which represents the continuum instability criterion developed on the basis of extremum principles of irreversible thermodynamics as applied to large plastic flow given by another dimensionless parameter[3, 5, 6]:

$$\xi(\dot{\varepsilon}) = \frac{\partial \ln[m/(m+1)]}{\partial \ln \dot{\varepsilon}} + m \tag{3}$$

Unstable flow is predicted when $\xi(\dot{\varepsilon}) < 0$. The variation of $\xi(\dot{\varepsilon})$ with temperature and strain rate constitutes the instability map which is superimposed over the power dissipation map to delineate the unstable flow regime. The processing map exhibits domains with local efficiency maxima representing specific microstructural mechanisms as well as regimes of flow instabilities.

The technique of processing map has been generally applied to process of magnesium alloys. Some processing maps of magnesium alloy can be obtained from the reference, such as magnesium (as-cast and extruded)[7], Mg-2Zn-1Mn (as-cast, homogenized and forged)[7, 8], AZ31B as-cast [9] and some Mg-Li alloys[7, 10]. All these processing maps have an instructive purpose to draw up plastic working process of magnesium alloys. While the processing maps of AZ31B magnesium alloy extruded have never seen from reference, so the processing maps of it were calculated and analyzed in this paper.

2 EXPERIMENTAL

The material used for compression tests was commercial grade AZ31B magnesium alloy as extruded. The chemical composition is given in Table 1. The initial microstructure of the specimen is

① **Foundation item:** Project(2001AA351050) supported by the National High-Tech Research and Development Program of China
Received date: 2004－11－05; **Accepted date:** 2005－01－24
Correspondence: HUANG Guang-sheng, PhD; Tel: +86-23-66978697; E-mail: gshuang@cqu.edu.cn

shown in Fig. 1, which is an equiaxed grain structure with an average grain diameter of about 18 μm.

Table 1 Composition of AZ31B magnesium alloy (mass fraction, %)

Al	Zn	Mn	Si	Cu	Fe	Ni
3.28	1.09	0.32	0.019	0.0053	0.005	0.004

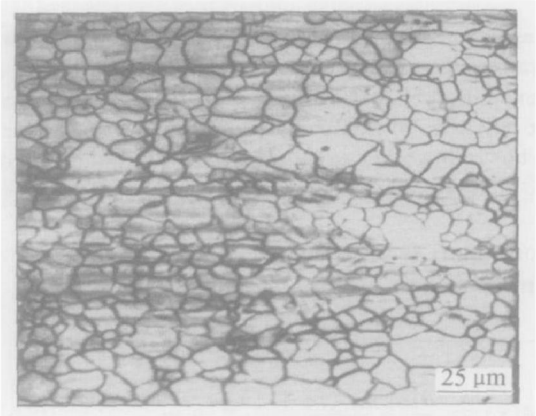

Fig. 1 Microstructure of AZ31B magnesium alloy as extruded

To investigate the hot workability and microstructure evolution, compression tests were performed in the temperature range between 200 ℃ and 400 ℃ with 50 ℃ intervals and the strain rate range between 10^{-3} s^{-1} and 1 s^{-1}. Compression test specimens of 12 mm in height and 10 mm in diameter were machined from hot extruded rod. All the tests were performed on the Gleeble-1500D thermal mechanical simulator. Before deformation, the rate of temperature rise was 1 ℃/s and the holding time of heat preservation was 5 min. Tantalum foil of 0.1 mm thickness was used between the specimen and dies to avoid sticking of the specimen to the dies. To observe the evolution of microstructure during compression tests, the compression-tested specimens were frozen by spray water as soon as the deformation completed. The specimens were sectioned in parallel to the stress axis for optical microscopy.

3 RESULTS AND DISCUSSION

3.1 High-temperature stress-strain behaviour

Typical true stress—true strain curves obtained at a representative strain rate of 0.1 s^{-1} and at different temperatures are shown in Fig. 2. Typically, the flow stress increases to a maximum and then decreases to a steady state. Such flow behavior is characteristic for hot working by dynamic recrystallization. In more detail, specific differences in the shape of the curves are evident. At low temperatures or high strain rates the flow curve exhibits high peak stress (σ_p) at a high peak strain (ε_p) and insignificant work softening is more pronounced. At high temperatures or low strain rates steady state is attained after small σ_p and ε_p with little softening.

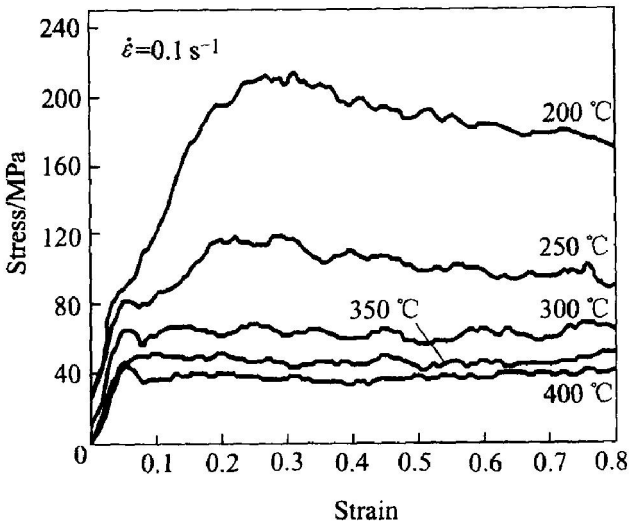

Fig. 2 Curves of stress—strain

3.2 Processing map

The processing map is obtained at different strains on the basis of the flow stress data at different temperatures and strain rates. Firstly, according to Eqn. (2), strain rate sensitivity at different temperatures and strain rates and constant strain can be obtained by functional relation between $\ln\sigma$ and $\ln\dot{\varepsilon}$ matching by cubic spline function. Table 2 lists m value of AZ31B magnesium alloy at the strain of 0.2. Then, power dissipation map can be plotted through efficiency of power dissipation that can be calculated by Eqn. (1). In a similar way, instability map can be plotted by the continuum criterion given by Eqn. (3). The processing maps are obtained by a superimposition of the instability maps over the power dissipation maps.

Table 2 m value of AZ31B magnesium alloy at strain of 0.2

$\dot{\varepsilon}$/ s^{-1}	t/ ℃				
	200	250	300	350	400
0.001	0.07	0.04	0.11	0.42	0.30
0.01	0.09	0.24	0.18	0.11	0.18
0.1	0.14	0.26	0.23	0.12	0.16
0	0.06	0.11	0.25	0.43	0.22

The processing map at a strain of 0.2 and in the temperature range of 200 – 400 ℃ with strain rate range of 0.001 – 1 s^{-1} for as extruded magnesium AZ31B alloy is shown in Fig. 3. The region of

flow instability as predicted by the continuum criterion given by Eqn. (3) is delineated by shaded region. The power dissipation maps show contours of constant efficiency of power dissipation, which represent the relative rate of entropy production occurring in the material due to microstructural dissipation[11, 12]. They can also be termed as microstructural trajectories since they actually represent the rate of change of microstructure occurring during hot deformation[13, 14].

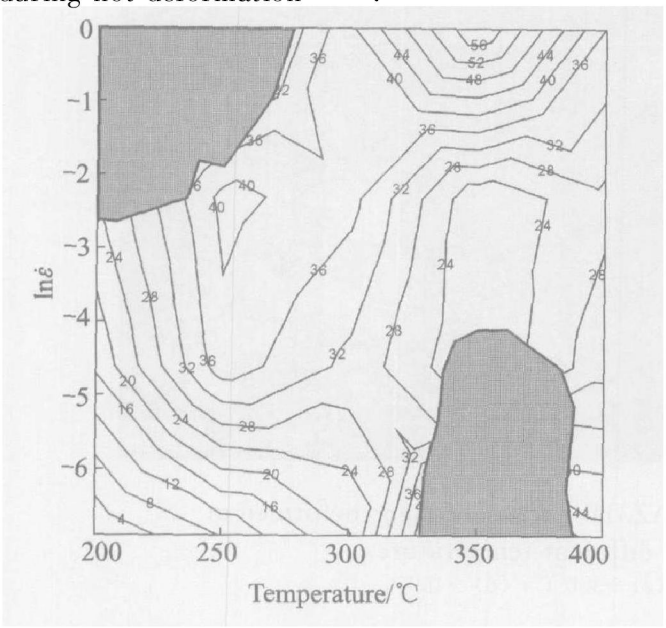

Fig. 3 Processing map for AZ31B magnesium alloy at strain of 0.2
(Contour numbers represent percent efficiency of power dissipation; shaded region corresponds to flow instability)

The map exhibits flow instabilities as two domains, one is at lower temperatures and higher strain rates, and the other is at higher temperatures and lower strain rates. At higher strains (e.g. 0.4, Fig. 4), the map also exhibits two domains as explained above, while the domains at lower temperatures and higher strain rates broaden to higher strain and lower temperatures.

The map at a strain of 0.2 exhibits one domain at a temperature of 250 ℃ and a strain rate of 0.01 s^{-1} with a maximum efficiency of power dissipation of about 40%. As the strain increases, this domain gives rise to another domain with a higher efficiency (44% at a strain of 0.4).

Simultaneously, another domain also appears with a peak efficiency of about 56% occurring at about 350 ℃ and strain rate of 1 s^{-1}. When the strain beyond 0.4, this domain has a temperature range of beyond 300 ℃. This domain is expected to happen in a hot process, such as hot rolling, hot extrusion and hot forging. AZ31B magnesium alloy has poor ductility because of the hexagonal close packed(HCP) structure, so the raw material for

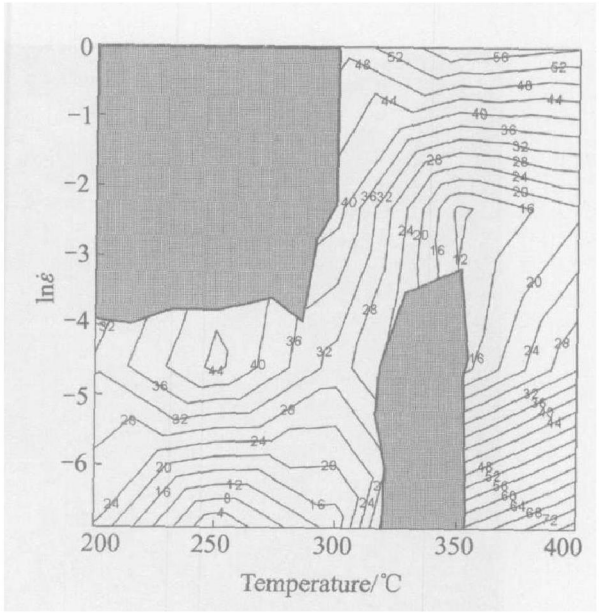

Fig. 4 Processing map for AZ31B magnesium alloy at strain of 0.4
(Contour numbers represent percent efficiency of power dissipation; shaded region corresponds to flow instability)

subsequent hot rolling, hot extruding or hot forging obtained by extrusion. For example, Chang et al[15] reported that an 203.2 mm in diameter ingot was first processed to a plate of 100 mm in width and 2 mm in thickness by indirect extrusion method, and then the 2 mm thickness plate was heated up to 400 ℃, subsequently reduced down to 0.5 – 1.3 mm.

Furthermore, there is high efficiency of power dissipation at temperature beyond 350 ℃ and strain rate of 0.001 s^{-1}. Such domains suggest the occurrence of superplastic deformation. The m value is greater than or equal to 0.3 from Table 2 in this region, which is in conformity to the superplasticity characteristic of strain rate sensitivity index. For instance, Watanabe et al[16] reported that they obtained about 200% of elongation-to-failure at temperature of 400 ℃ and strain rate of 1×10^{-3} s^{-1} with AZ31B alloy extruded rod, and elongation-to-failure would be up to 420% with the strain rate decreasing to 1×10^{-4} s^{-1}.

The microstructures shown in Fig. 5 also indicate the validity of the processing maps. According to Fig. 4, the two instable microstructures (Figs. 5 (a) and (b)) present fall in the instable regions. The flow instability takes place mainly because of nonhomogeneous grain boundary deformation. The deformation microstructures of AZ31B magnesium alloy at this deformation condition are remarkable necklace structures and non-uniform markedly. The microstructures are undesirable in obtaining consistent mechanical properties and hence should be avoided in processing. Whereas the two stable

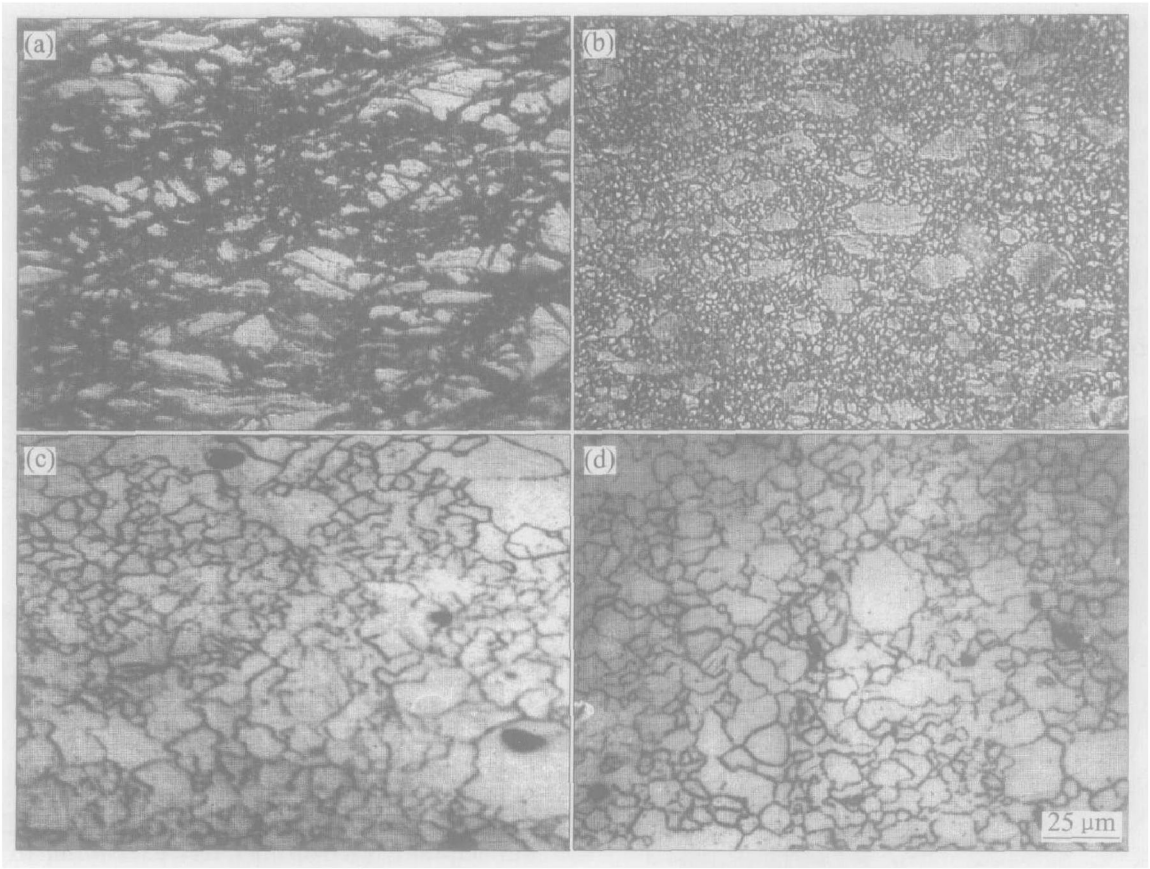

Fig. 5 Microstructures obtained on AZ31B alloy specimens deformed at strain rate of 0.1 s^{-1} and different temperatures
(a) —200 ℃; (b) —250 ℃; (c) —350 ℃; (d) —400 ℃

microstructures(Figs. 5(c) and (d)) fall in the stable regions of the instability map (Fig. 4). Microstructural observations of the specimens deformed at instable regions are mainly incomplete recrystallization, while the stable microstructures are complete recrystallization.

4 CONCLUSIONS

1) The processing map of as extruded AZ31B magnesium alloy exhibits flow instabilities as two domains, one is at lower temperatures and higher strain rates, the other is at higher temperatures and lower strain rates.

2) The domain at beyond 300 ℃and strain rate of 1 s^{-1} appears with a peak efficiency of about 56% occurring. This domain is expected to happen in a hot process, such as hot rolling, hot extrusion and hot forging.

3) There is high efficiency of power dissipation at temperature beyond 350 ℃ and at strain rate of 0.001 s^{-1}. Such domains suggest the occurrence of superplastic deformation.

REFERENCES

[1] Jain V K, Jata K V, Rioja R J, et al. Processing of an experimental aluminum-lithium alloy for controlled microstructure[J]. Journal of Materials Processing Technology, 1998, 73: 108 - 118.

[2] Bozzini B, Cerri E. Numerical reliability of hot working processing maps[J]. Materials Science and Engineering, 2002, A328: 344 - 347.

[3] Prasad Y V R K, Seshacharyulu T. Processing maps for hot working of titanium alloys[J]. Materials Science and Engineering, 1998, A243: 82 - 88.

[4] Kridli G K, El-Gizawy A S, Lederich R. Development of process maps for superplastic forming of weldalite (tm) 049[J]. Materials Science and Engineering, 1998, A244: 224 - 232.

[5] Park N K, Yeom J T, Na Y S. Characterization of deformation stability in hot forging conventional Ti-6Al-4V using processing maps[J]. Journal of Materials Processing Technology, 2002, 130 - 131: 540 - 545.

[6] Prasad Y V R K, Sasidhara S, Sikka V K. Characterization of mechanisms of hot deformation of as-cast nickel aluminide alloy[J]. Intermetallics, 2000, 8: 987 - 995.

[7] Avedesian M M, Baker H. ASM Specialty Handbook: Magnesium and Magnesium Alloys [M]. Ohio: ASM International, 1999.

[8] Sivakesavam O, Prasad Y V R K. Hot deformation behaviour of as-cast Mg-2Zn-1Mn alloy in compression: a study with processing map [J]. Materials Science and Engineering, 2003, A362: 118 - 124.

[9] WANG Ling-yun, FAN Yong-ge, HUANG Guang-sheng, et al. Research on plastic deformation at elevated temperature and processing maps of magnesium alloy [J]. The Chinese Journal of Nonferrous Metals,

2004, 14(7): 1068 - 1072. (in Chinese)

[10] Sivakesavam O, Prasad Y V R K. Characteristics of superplasticity domain in the processing map for hot working of as-cast Mg-11.5Li-1.5Al alloy [J]. Materials Science and Engineering, 2002, A323: 270 - 277.

[11] Sundar R S, Sastry D H, Prasad Y V R K. Hot workability of as-cast Fe3Al-2.5% Cr intermetallic alloy[J]. Materials Science and Engineering, 2000, A347: 86 - 92.

[12] Prasad Y V R K, Sastry D H, Deevi S C. Processing maps for hot working of a P/M iron aluminide alloy [J]. Intermetallics, 2000, 8: 1067 - 1074.

[13] Gronostajski Z. The deformation processing map for control of microstructure in CuAl9.2Fe3 aluminium bronze [J]. Journal of Materials Processing Technology, 2002, 125 - 126: 119 - 124.

[14] Narayana M S V S, Nageswara R B. On the flow localization concepts in the processing maps of IN718 [J]. Materials Science and Engineering, 1999, A267: 159 - 161.

[15] CHANG Tien-chan, WANG Jian-yi, Chia-Ming O, et al. Grain refining of magnesium alloy AZ31 by rolling [J]. Journal of Materials Processing Technology, 2003, 140: 588 - 591.

[16] Watanabe H, Tsutsui H, Mukai T, et al. Superplastic behavior in commercial wrought magnesium alloys [J]. Materials Science Forum, 2000, 350 - 351: 171 - 176.

(Edited by LI Xiang-qun)